



1 **Rainfall redistribution in subtropical Chinese forests changes over 22**

2 **years**

3 Wanjun Zhang^{a,b}, Thomas Scholten^c, Steffen Seitz^c, Qianmei Zhang^{a,b}, Guowei Chu^{a,b}, Linhua

4 Wang^{a,b}, Juxiu Liu^{a,b,*}

5

6 ^a*Key Laboratory of Vegetation Restoration and Management of Degraded Ecosystems, South China*

7 *Botanical Garden, Chinese Academy of Sciences, Guangzhou, 510650, China*

8 ^b*Guangdong Provincial Key Laboratory of Applied Botany, South China Botanical Garden, Chinese*

9 *Academy of Sciences, Guangzhou, 510650, China*

10 ^c*Soil Science and Geomorphology, Department of Geosciences, University of Tübingen, Tübingen,*

11 *72070, Germany*

12

13 * Correspondence to: Juxiu Liu (ljxiu@scbg.ac.cn)



14 **Abstract**

15 Rainfall redistribution through the vegetation canopy plays a key role in the
16 hydrological cycle. Although there have been studies on the heterogeneous patterns of
17 rainfall redistribution in some ecosystems, the understanding of this process in different
18 stages of forest succession remains insufficient. Therefore, this study investigated the
19 change tendency of rainfall redistribution and rainwater chemistry in a subtropical
20 succession forest area in South China, based on 22 years (2001–2022) of monitoring
21 740 valid rainfall events. Results showed that at the event scale throughfall ratio showed
22 in order broadleaf forest (BF) < mixed forest (MF) < pine forest (PF), and stemflow
23 ratio showed in order BF > MF > PF. At the interannual scale, annual gross rainfall
24 considerably shifted over time, which directly induced the variable accumulation of
25 annual throughfall and annual stemflow. In the last 22 years, annual variability of
26 throughfall presented in order MF (*CV*, 9.7%) < BF (15.6%) < PF (16.1%), and annual
27 variability of stemflow presented in order MF (*CV*, 38.6%) < PF (50.9) < BF (56.2%).
28 The spatial variability of stemflow was always greater than that of throughfall. Besides,
29 the difference of rainwater chemistry fluxes (TN, TP and K⁺) among the three forest
30 types were found and they changed over time. Throughfall was characterized with high
31 chemistry fluxes compared to open rainfall followed by stemflow. On average, TN and
32 TP fluxes of throughfall presented in order BF < MF < PF, while K⁺ flux of throughfall
33 presented in order BF > MF > PF. The above results indicated that the patterns of
34 rainfall redistribution often changed over time. The event-scale accumulation of
35 throughfall and stemflow potentially induced the interannual-scale variability. Both
36 water volume and chemistry of throughfall and stemflow depended on the effect of
37 rainfall and forest factors. This study provided insight into the rainfall redistribution
38 process by linking the long-term changing of rainfall pattern and subtropical forest
39 succession sequence.

40 **Keyword:** throughfall, stemflow, variability, forest types, long-term



41 **1. Introduction**

42 In recent years, there has been on-going concern about the potential impacts of
43 climate change on forest ecosystems, particularly in terms of rainfall input associated
44 to water resource (Reynaert et al., 2020; Grossiord et al., 2017; Bruijnzeel et al., 2011;
45 Leuzinger and Körner, 2010). Numerous studies have documented rainfall regimes and
46 their effect on the water cycle in different regions of the world, including spatial and
47 temporal changes in the amount, intensity, and frequency (Brasil et al., 2018; Ponette-
48 González et al., 2010). Meanwhile, these variables in rainfall refer to the redistribution
49 of rainfall into canopy interception, throughfall and stemflow, being important
50 components of ecosystems hydrological processes (Germer et al., 2010; Levia and Frost,
51 2006; Loustau et al., 1992). Rainfall redistribution patterns can impact the
52 biogeochemistry cycle by affecting soil moisture, which in turn affects the activity of
53 soil microorganisms that decompose organic matter (Tonello et al., 2021a; Junior et al.,
54 2017; Van Stan II and Pypker, 2015). The study of Sun et al. (2023) verified that
55 throughfall reduction significantly affected soil carbon cycle in a subtropical forest.
56 Therefore, understanding the roles of rainfall redistribution in the water cycle is
57 essential.

58 Rainfall redistribution, as the partitioning into interception loss, throughfall and
59 stemflow, is an important hydrological process that regulates water and nutrient cycling
60 in forest ecosystems. Interception loss refers to the part of the event rainfall intercepted
61 by the canopy, accounting for about 10%–30% of gross rainfall depending on the
62 studied forest canopy, such as shrub (Zhang et al., 2015), mixed broadleaf (Yan et al.,
63 2003), pine (Loustau et al., 1992). This portion of the rainwater evaporates directly back
64 into the atmosphere. Later on, the remaining rainwater reaches the ground either as
65 throughfall or stemflow. Throughfall is a critical component of rainfall redistribution,
66 and it on average contributes to approximately 60%–90% of the gross rainfall on the
67 floor in forests, shrubland or cropland. (Zhang et al., 2023; Zhang et al., 2021; Brauman
68 et al., 2010; Marin et al., 2000). Raindrops coalesce or splash on canopy leaf surfaces,
69 generating spatially different throughfall volume and raindrop kinetic energies which
70 can be larger or lower than that of open rainfall (Levia et al., 2019; Goebes et al., 2015).
71 Stemflow, the left rainwater flowing bottomwards along the plant stem or trunk, often
72 accounts for only a small proportion (0–12%) of rainfall (Niu et al., 2023; Yue et al,
73 2021; Llorens and Domingo 2007). Nevertheless, stemflow inputs can be important as
74 hot spots for near-trunk soils, inducing water and nutrient enrichment and deep



75 infiltration, but also erosion (Zhao et al., 2023; Llorens et al., 2022). It can funnel more
76 water than open rainfall on an equivalent area and contributes to 10% of the annual soil
77 water input (Levia and Germer, 2015; Chang and Matzner, 2000). Throughfall and
78 stemflow restrict water input to the soil layer, thereby affecting soil moisture conditions,
79 runoff generation and water and nutrient cycling (Lacombe et al., 2018; Klos et al.,
80 2014).

81 The proportions of rainfall redistribution are generally driven by meteorological
82 conditions (e.g., rainfall amount, intensity, duration) and vegetation cover (e.g., canopy
83 structures, tree characteristics) (Tonello et al., 2021a; Sun et al., 2018; Muzyło et al.,
84 2012; Nanko et al., 2006). For meteorological conditions, numerous studies have
85 documented that throughfall volume and stemflow volume increase with increasing
86 gross rainfall and intensity (Ji et al., 2023; André et al., 2011). The ratios of throughfall
87 and stemflow were both characterized with logarithmically increasing with rainfall,
88 tending to be quasi-constant for heavy rainfall events (Zhang et al., 2021; Liu et al.,
89 2019). This was also synchronously related to the gradual saturation of the canopy
90 which limited the ratios of rainwater partitioning (Carlyle-Moses et al., 2004). Besides,
91 differences of water volume spatially exist from place to place. The spatial variability
92 (expressed as a coefficient of variation) of throughfall volume is generally higher for
93 small rainfall events (< 10 mm) than that for heavy rainfall events (Germer et al., 2006;
94 Price et al., 1997).

95 Rainfall redistribution among different plant species can vary significantly due to
96 differences in the structure and characteristics of their canopies. In special, some of the
97 key factors determine the redistribution of rainfall, for example, leaf area index (LAI),
98 leaf shapes and orientations can affect the amount of intercepted loss and throughfall
99 (Zhang et al., 2021; Goebes et al., 2015; Keim et al., 2006). The diameter at breast
100 height (DBH), bark type and orientation of trunks/stems and branches influence the
101 amount of stemflow (Levia et al., 2015; Livesley et al., 2014; Germer et al., 2010). For
102 each of the rainfall partitioning fluxes, their responses to the influential predictors often
103 show high variation. A modelling study of rainfall partitioning in China explained that
104 throughfall was best represented by mean tilt angle (MTA), followed by DBH.
105 Subsequently, DBH was the dominant predictor for stemflow, followed by LAI and
106 bark texture (Zhang et al., 2023). Due to these factors, rainfall redistribution presented
107 different degrees of spatial variability. This variability (expressed as coefficient of
108 variation) decreased with increasing rainfall amount and intensity, consequently



109 tending to be quasi-constant (Germer et al., 2006). Besides, at interannual scale, ratios
110 of rainfall redistribution are driven by annual canopy structures. The study of Niu et al.
111 (2023) documented that annual throughfall ratio gradually increased, while annual
112 stemflow ratio and interception loss ratio decreased with increasing thinning intensity
113 in shrub plantation. Meanwhile, annual changes of rainfall events (amount and intensity)
114 reinforced the time instability of throughfall spatial variability (Rodrigues et al., 2022).
115 Overall, the rainfall-canopy interactions play a key role in rainfall redistribution
116 processes and further affect the water cycle in many ecosystems.

117 Vegetation canopy is the functional interface between ecosystem and atmospheric
118 wet deposition (Van Stan II and Pypker, 2015). The leaf and trunk/stem, acting as a
119 filter, alter rainwater chemical concentrations via leaching and depositing processes. As
120 a result, throughfall and stemflow exhibit high chemical concentrations compared to
121 the open rainfall (Jiang et al., 2021; Zimmermann et al., 2007). For instance, in a Chinese
122 pine plantation, the volume weighted mean concentrations of NH_4^+ and NO_3^-
123 in throughfall were significantly higher than those in open rainfall (Wang et al., 2023).
124 Stemflow ion fluxes (e.g., K^+) from deciduous tree species were greater than those for
125 evergreen tree species because of the differences in bark morphology and branch
126 architecture (Su et al., 2019). Moreover, it is also common that throughfall and
127 stemflow chemistry fluctuated seasonality with the shifts in rainfall regime and leaf
128 growth (Turpault et al., 2021; Siegert and Levia, 2014; Staelens et al., 2007). A large
129 number of elements required by plants are mainly N, P, K, Ca and Mg. In general, N, K
130 and Ca are the most important inputs to forest ecosystem, and P is the least. Phosphorus
131 (P) is considered to be a limiting nutrient element in tropical and subtropical forests.
132 The long-term productivity of vegetation depends on the input of atmospheric P.
133 Besides, the increasing trend in seasonal drought and atmospheric nitrogen (N)
134 deposition in subtropical areas of China were reported (Zhou et al., 2011), and may
135 inhibit the growth of plant and affect productivity and functioning of forest ecosystems
136 (Wu et al., 2023; Borghetti et al., 2017). Therefore, the important significance of
137 atmospheric precipitation to the ecosystem can also be seen from the amount of element
138 cycling, and canopy leaching also plays an important role in the chemistry cycle of
139 forest ecosystems.

140 Although there have been studies on the spatio-temporal variability of rainfall
141 redistribution, most of these are limited to data of short-term monitoring over one-two
142 years or several months (Liu et al., 2019; Ziegler et al., 2009; Carlyle-Moses, 2004;



143 Marin et al., 2000). There are few studies exceeding several years experiments and
144 focusing on forest structural changes and rainwater interception (Grunicke et al., 2020;
145 Shinohara et al., 2015; Jackson, 2000). Long-term field monitoring studies are
146 considered to be valuable to gain insight into the temporal dynamics of forest
147 hydrological processes (Rodrigues et al., 2022; Sun et al., 2023; Levia and Frost, 2006).
148 Such studies can also contribute to identify patterns and trends in rainfall redistribution,
149 which is essential for predicting the long-term effect of water resource change on forest
150 ecosystems.

151 Therefore, in this study, we focus on the changing characteristics of throughfall
152 and stemflow in a subtropical forest succession sequence (pine forest → mixed forest →
153 monsoon evergreen broadleaf forest), based on long-term monitoring. Specifically, the
154 objectives are to analyze: (1) the changes of water volume of throughfall and stemflow
155 among the three forests, (2) the changes of water chemistry (TN, TP, K⁺) of rainfall,
156 throughfall and stemflow among the three forests. We hypothesize that: (1) both
157 throughfall and stemflow in the broadleaf forest were characterized with high
158 variability compared to mixed forest followed by pine forest, (2) chemistry flux of
159 throughfall and stemflow changed over time with in order broadleaf forest > mixed
160 forest > pine forest. We aim to assess the variability of forest hydrological processes
161 from a long-term perspective to help predict future dynamic trends of water resources
162 in subtropical forest ecosystems.

163

164 **2. Materials and Methods**

165 *2.1. Study site*

166 This study was conducted at the Dinghushan Biosphere Reserve (23°09' 21" N ~
167 23°11' 30" N, 112°30' 39" E ~ 112°33' 41" E) located in Zhaoqing City, South China.
168 Dinghushan catchment consists of two streams both with 12 km length, which flow into
169 the West River (the main trunk of the Pearl River). According to the Köppen-Geiger
170 climate classification (Kottek et al., 2006), the study area belongs to tropical monsoon
171 climate (Cwa) with pronounced wet (April-September) and dry season (October-
172 March). The average annual temperature is 20.9 °C, and the annual rainfall and
173 evaporation are 1900 mm and 1115 mm, respectively. Dinghushan Biosphere Reserve
174 is covered with a complete horizontal succession series of three types of subtropical
175 forest, which is highly representative of the region (Zhou et al., 2011). Monsoon



176 evergreen broadleaf forest (BF) is 400 years old with typical tree species including
177 *Castanopsis chinensis* (Spreng.) Hance, *Schima superba* Gardner & Champ.,
178 *Cryptocarya concinna* Hance, etc. The mixed pine/broadleaf forest (MF) is a natural
179 succession with a coniferous broadleaf ratio of about 4:6, and 70–80 years old. The
180 main broadleaf tree species are *Schima superba* Gardner & Champ., *Castanopsis*
181 *chinensis* (Spreng.) Hance, and the coniferous species *Pinus massoniana* Lamb. The
182 pine forest (PF) planted before 1960 belongs to the primary succession community
183 where *Pinus massoniana* Lamb forms the only tree layer.

184

185 2.2. Gross rainfall, throughfall and stemflow monitoring

186 Atmospheric rainfall data was collected at Dinghushan Automatic Meteorological
187 Station from 2001–2022. The resolution of data recording was ± 0.2 mm with a time
188 interval of 10 min. The raw data comprised annual rainfall amounts, as well as single
189 rainfall events with throughfall and stemflow measurements. Throughfall and stemflow
190 were collected in all three forest types and synchronously measured. Devices with
191 cross-shaped collectors (1.25 m^2) attached to reservoirs (1000 L) at the bottom were
192 used to collect throughfall. Three throughfall devices were randomly installed in each
193 forest field. Half-shell plastic tubes were installed around tree trunks attached to
194 reservoirs (1000 L) at the bottom to collect stemflow. A total of 24 trees with six tree
195 species were selected to measure stemflow volume. In detail, four tree species were
196 selected in the broadleaf forest, including *Acmena acuminatissima* (Blume) Merr. et
197 Perry (SF1), *Cryptocarya chinensis* (Hance) Hemsl. (SF2), *Gironniera subaequalis*
198 Planch. (SF3), *Schima superba* Gardn. et Champ. (SF4), with 3 repetitions respectively.
199 Three tree species were selected in the mixed forest, including *Castanea henryi* (Skam)
200 Rehd. et Wils. (SF5), *Schima superba* Gardn. et Champ. (SF6), *Pinus*
201 *massoniana* Lamb. (SF7), with 3 repetitions respectively. In the pine forest, *Pinus*
202 *massoniana* Lamb. (SF8) was selected as the monitoring subject with 3 repetitions.
203 Growth indicators of the selected trees have been recorded every five years since 2000:
204 tree height (m), DBH (cm), and crown area (CA, m^2). Forest structures have been
205 measured every five years since 2000: plant density (tree, shrub and herb), forest
206 canopy coverage (%) and LAI.

207



208 *2.3. Rainwater chemistry measurement*

209 For the measurement of rainwater chemistry, rainwater samples were from 2000,
210 2010 and 2022 in Dinghushan area. The samples of open rainfall, throughfall and
211 stemflow were manually collected for every one-month period, respectively. The
212 samples of open rainfall and throughfall were collected with three repetitions,
213 respectively and stemflow with four repetitions in the broadleaf forest, three repetitions
214 in the mixed forest and three repetitions in the pine forest. In total, 792 rainwater
215 samples (108 open rainfall, 324 throughfall and 360 stemflow) were collected.

216 Rainwater samples were defrosted and filtered through 0.45 μm polypropylene
217 membranes. Concentrations of total nitrogen (TN) and total phosphorus (TP) were
218 measured using ultraviolet spectrophotometer (Lambda 25, Perkin-Elmer), and ion
219 potassium (K^+) was measured using an inductively coupled plasma optical emission
220 spectrometer (Optima 2000, Perkin-Elmer), respectively. The origin data of TN, TP and
221 K^+ were processed into annual flux and monthly values by weighted average method,

$$222 \quad C = \frac{\sum C_i * V_i}{\sum V_i} \quad (1)$$

223 where C_i and V_i are the concentrations of ions (mg L^{-1}) and water sample volume (L) in
224 each rainfall event, respectively.

225

226 *2.4. Statistical analysis and calculations*

227 The differences in throughfall and stemflow among different forests were assessed
228 using analysis of variance (ANOVA), followed by a Tukey test for multiple
229 comparisons between means. All statistical procedures were conducted with $\alpha = 0.05$
230 threshold for significance, in the IBM SPSS statistics 22.0 software (IBM Inc.).

231

232 **3. Results**

233 *3.1. Open rainfall*

234 Based on the 22 years rainfall dataset from the Dinghushan area, annual gross
235 rainfall ranged between 1370.0 and 2361.1 mm. In detail, approximately 80% of gross
236 rainfall appeared in the rainy season (April–September). Anomaly were revealed in the
237 temporal variability (coefficient of variation, CV of 16.6%) in annual rainfall (Fig. 1a).
238 In details, some remarkable negative values in 2003-2005, 2007, 2011 and 2021 and
239 positive values in 2006, 2008, 2015, 2018 and 2019 were found. Anomaly varied at -
240 426.4–476.8 mm and -258.0–471.4 mm in the rainy season and dry season, respectively.



241 By comparison, dry season experienced greater variation with CV of 40.4% than rainy
242 season with CV of 21.7%. Besides, annual raining days obviously tended to decrease
243 over time from 2012 to 2021(Fig. 1b). Based on five rainfall classifications, it was
244 shown among 22 years that rainfall <10 mm account for about 68.5% of total raining
245 days (2856), while rainfall >50 mm account for about 4.9%.

246

247 3.2 Variability of throughfall

248 Rainfall redistribution (throughfall + stemflow, TS) among the three forests all
249 experienced differing magnitude during 22 years (Fig. 2). Anomalies of TS revealed
250 that TS received below normal value similar with open rainfall. For throughfall ratio, it
251 varied significantly both at the event and interannual scales (Fig. 3a, b and c). The
252 median of annual throughfall ratio in the broadleaf forest varied between 60% and 120%
253 with CV of 13% from 2001–2022. The median of throughfall ratio in the mixed pine
254 and broadleaf forest varied between 80% and 110% with a CV of 10%. The median of
255 throughfall ratio in the pine forest varied between 59% and 110% with a CV of 11%.
256 Therefore, throughfall ratio was characterized by a relatively low variability over
257 annual-time scale ($CV < 15\%$). Besides, some differences of throughfall ratio were
258 found among the three forest types based on rainfall classifications. For rainfall events
259 < 10 mm, throughfall ratio range in the broadleaf forest was 35%–70%, while in the
260 other two forest types it was 20%–85% (Fig. 3d). The mean value of throughfall ratio
261 was relatively small in the broadleaf forest (53.9%), though no significant difference
262 among the three forests ($P > 0.05$) were detected. For rainfall events <50 mm, no
263 significant difference of throughfall ratio among the three forest types was found ($P >$
264 0.05). However, the average values of throughfall ratio in the pine forest and the mixed
265 forest were both significantly larger than that in the broadleaf forest for rainfall
266 events >50 mm.

267 CV values of throughfall based on all the rainfall event classifications were drawn
268 in the Fig. 4a. Results showed that median CV of throughfall in the pine forest (15.2%)
269 was lower than that for the broadleaf forest (21.7%) and for the mixed forest (26.3%)
270 for rainfall events <10 mm. For rainfall events >10 mm, small differences of median
271 CV among the three forest types were shown. Meanwhile, CV values decreased with
272 the increasing rainfall events, eventually falling to 3.5%–4.3%. Besides, CV values of
273 throughfall based on interannual scale were drawn in the Fig. 5a, b and c. Annual CV
274 values among different forest types showed different fluctuations over time. The



275 medians of CV in annual, rainy and dry seasons presented different order in different
276 years. According to linear fitting, significant negative correlations were found in the
277 median of CV_{TF} in the mixed forest over time ($r = 0.63$, $P < 0.01$). In addition, fitting
278 result of in total 740 rainfall events in 22 years showed that CV values of throughfall
279 significantly decreased with increasing gross rainfall (Fig. S1).

280

281 3.3 Variability of stemflow

282 Among 22 years, the median of annual stemflow ratio in the broadleaf forest varied
283 between 1.3% and 5.4% with a CV of 56.2%. The stemflow ratio of mixed forest varied
284 between 1.5% and 4.4% with a CV of 38.6%. In the pine forest, it varied between 0.3%
285 and 1% with a CV of 50.9%. This indicated that the stemflow ratio was characterized
286 by an extremely high variability over time. Same to the seasonal throughfall ratio, the
287 medians of stemflow ratio in annual, rainy and dry seasons presented different orders
288 in different years. Besides, the stemflow ratio significantly changed among tree species
289 and among rainfall classifications (Fig. 3e). By comparison, stemflow ratios of the SF1
290 and SF2 trees in the broadleaf forest were both higher in all the tree species for the
291 rainfall events < 50 mm. However, for strong events (> 50 mm), the stemflow ratio of
292 the SF5 tree in the mixed forest was highest for all tree species, followed by the trees
293 in the broadleaf forest. For all the rainfall events, the stemflow ratio of SF7 in the mixed
294 forest and SF8 in the pine forest were both lower than that for other tree species.

295 CV values of stemflow based on rainfall event classifications were drawn in the
296 Fig. 4b. By comparison, stemflow varied more than those of throughfall across rainfall
297 events, with CV_{SF} values of 25%–130%. Median CV of stemflow in the pine forest was
298 always lower (45%–68%) than that for the other two forest types (56%–120%). CV
299 values of stemflow based on interannual scale changed over time among different forest
300 types (Fig. 5d, e and f). The medians of CV_{SF} in annual, rainy and dry seasons presented
301 different order in different years. By comparison, CV_{SF} was always greater than CV_{TF} ,
302 and interannual fluctuation of CV_{SF} was also stronger than CV_{TF} . According to linear
303 fitting, significant negative correlations were found in the median of CV_{SF} in the
304 broadleaf forest over time ($r = 0.73$, $P < 0.001$). In addition, fitting result of in total
305 740 rainfall events in 22 years showed that CV values of stemflow both significantly
306 decreased with increasing gross rainfall (Fig. S1).

307



308 *3.4. Rainwater chemistry*

309 Rainwater (open rainfall, throughfall and stemflow) chemical properties (TN, TP
310 and K⁺ concentration) were measured in the three forest types, respectively. All of TN,
311 TP and K⁺ values presented in order stemflow > throughfall > open rainfall (Fig. 6a, b
312 and c). However, changes of TN, TP and K⁺ were different for the three forest types
313 among 2000, 2010 and 2022. For instance, in 2000 and 2010, TN values of throughfall
314 and stemflow decreased for both in order of pine forest > mixed forest > broadleaf forest,
315 while no such result could be confirmed in 2022. Similarly, TP values of throughfall in
316 broadleaf forest was 1.3 times higher than that in pine forest in 2022, while TP values
317 in pine forest was 6.8 time than that in broadleaf forest in 2000. K⁺ values of stemflow
318 in 2010 (6.76 mg L⁻¹) and 2022 (6.22 mg L⁻¹) were higher for broadleaf forest than
319 those for pine forest (3.76 mg L⁻¹ and 2.46 mg L⁻¹), which was different from that in
320 2022.

321 TN, TP and K⁺ fluxes of stemflow were < 10 kg ha⁻¹ a⁻¹, 0.2 kg ha⁻¹ a⁻¹, 6 kg ha⁻¹
322 a⁻¹, respectively, all lower than those of throughfall and open rainfall (Fig. 7d, e and f).
323 In the 2000, 2010 and 2022, TN flux (39.4–87.4 kg ha⁻¹ a⁻¹) was 1.2–1.8 times greater
324 than that of open rainfall, 3.3–28.0 times greater than that of stemflow. TP flux (1.1–
325 2.7 kg ha⁻¹ a⁻¹) was 1.0–2.3 times greater than that of open rainfall, 8.7–31.4 times
326 greater than that of stemflow. K⁺ flux (21.5–59.2 kg ha⁻¹ a⁻¹) was 2.2–8.1 times greater
327 than that of open rainfall, 2.2–26.8 times greater than that of stemflow. In addition, TN,
328 TP and K⁺ fluxes of stemflow increased with succession from primary to climax,
329 namely pine forest < mixed forest < broadleaf forest. Different from this, differences in
330 chemistry fluxes of throughfall was not found among different forests, neither among
331 different periods.

332 Besides, monthly chemistry concentrations in rainfall, throughfall and stemflow
333 showed distinct changes (Fig. 7). Monthly TN, TP and K⁺ concentrations of rainfall
334 were always lower than those of stemflow for all trees. Monthly TN, TP and K⁺ of
335 stemflow in the dry season were generally higher than in the rainy season. High monthly
336 TN concentrations of stemflow with SF6 of mixed forest and SF8 of pine forest were
337 found, especially in dry season with maximum TN concentrations of 27.59 mg L⁻¹ at
338 SF6 and 19.94 mg L⁻¹ at SF8, respectively. Differently, high monthly K⁺ concentration
339 of stemflow at SF4 in broadleaf forest was found, with in dry season maximum K⁺
340 concentration of 25.17 mg L⁻¹.



341

342 **4. Discussion**

343 *4.1. Open rainfall partitioned to throughfall and stemflow*

344 Studies in forests have confirmed that throughfall volume increased with
345 increasing gross rainfall at event scale, accounting for 60%–80% of gross rainfall (Ji et
346 al., 2023; André et al., 2011; Carlyle-Moses, 2004). This study, with 22 years of data,
347 showed that annual rainfall changed over long-time scale and for different rainfall
348 classifications (Fig. 1), which can directly affect annual throughfall. Throughfall ratio
349 changed over time and showed different fluctuations among different forests (Fig. 3).
350 During light rainfall events with rainfall amounts < 10 mm, a low proportion of
351 raindrops would reach the ground as throughfall, as the tree canopy intercepts almost
352 all the incoming raindrops. Specifically, high canopy coverage in broadleaf forest can
353 reinforce raindrop intercept (Brasil et al., 2018; Ponette-González et al., 2010),
354 consequently generating lower throughfall ratio than those in the mixed forest and pine
355 forest (Fig. 3). During moderate rainfall events (10–50 mm), given that the intercept
356 effect of the wetting tree canopy was weakened (Shinohara et al., 2015), throughfall
357 ratio was in a high and steady state. As the gross rainfall increases further (> 50 mm),
358 significant differences of throughfall ratio were found among the three forests.
359 Throughfall ratio was significantly lower in the broadleaf forest than those in the other
360 two forests. Likewise, such differences due to rainfall event class also appeared in other
361 forest studies with stands such as beech, pine in monocultures and mixed pine-beech
362 (Blume et al., 2022). Influenced by forest stand characteristics, throughfall therefore
363 indicated different forest water budget.

364 Stemflow ratio of forests were variably controlled by tree species, on average
365 accounting for about <10% of gross rainfall, even lower (<1%) (Sun et al., 2018; André
366 et al., 2008; Crockford and Richardson, 1990). In our study site, the lowest stemflow
367 (<1%) was collected in the pine forest, though weakly increasing with rainfall
368 classifications (Fig. 3). Stemflow ratio in broadleaf forest was maintained at 5%–10%
369 without the effect of rainfall amount seemingly. In detail, stemflow ratio of pine forest
370 (SF8) was significantly lower than those of broadleaf forest (SF1~4). And in the mixed
371 forest, broad-leaved trees (SF5 and SF 6) have larger stemflow than pine tree (SF7).
372 However, for some rainfall events, extraordinary low proportion of stemflow in the
373 broadleaf forest and extraordinary high proportion in the pine forest were caught. This



374 implied the role of rainfall conditions (e.g., intensity, duration) and tree species with
375 tree traits (e.g., branch angle), consistent with reported studies e.g., in evergreen forest
376 (Chen et al., 2019; Bruijnzeel et al., 2011) and pine forest (Crockford and Richardson,
377 1990). Moreover, ANOVA showed significant differences of stemflow ratio among tree
378 species and rainfall classifications ($P < 0.001$) (Table 1). This indicated that rainfall and
379 tree species simultaneously affect stemflow. Branch inclination angle, canopy cover,
380 tree height and DBH of tree species proved to be key factors in stemflow yield (Levia
381 et al., 2015).

382 Throughfall and stemflow were generally enriched in chemical concentration
383 compared with open rainfall due to leachable canopy/stem ion pools (Jiang et al., 2021;
384 Van Stan et al., 2017; Zimmermann et al., 2007). In our study, the concentration of K^+
385 in stemflow was 16 times higher than that in open rainfall and in throughfall reached
386 up to 11 times higher than open rainfall (Fig. 6). Similar results were also found in
387 artificial plantation (*Acacia mangium* and *Dimocarpus longan*) of South China (Shen
388 et al., 2013), in Oriental beech (*Fagus orientalis* Lipsky) trees in Northern Iran (Moslehi
389 et al., 2019), indicating strong K^+ leaching from canopy. Even so, throughfall was
390 generally characterized with high fluxes compared to open rainfall followed by
391 stemflow, it thus is the largest contributor to wet deposition. Meanwhile, TN flux of
392 throughfall was greatest in the pine forest in 2010, TP flux of throughfall was greatest
393 in the broadleaf forest in 2000, and K^+ flux of throughfall was greatest in the mixed
394 forest in 2010. It should be noted that the differences of rainwater chemistry shifted
395 over time among the three forests. Accordingly, throughfall and stemflow via canopy
396 and stem input soil is a significant contributor, and its long-term effect on ecosystems
397 needs more attention (Fan et al., 2021). After all, atmospheric wet deposition provides
398 nutrient requirement for ecosystems, but also imposes a considerable burden on the
399 ecosystems in general. For instance, N enrichment and P limitation have proven to have
400 different effect on soil carbon sequestration, microbial community composition and
401 forest productivity, especially in tropical and subtropical forest ecosystems with highly
402 weathered soils (Zheng et al., 2022; Li et al., 2016; Huang et al., 2012). Besides,
403 throughfall and stemflow was mainly characterized by low chemical concentrations in
404 the rainy season and high concentrations in the dry season. Primary reasons for seasonal
405 rainwater chemistry may be attributable to moisture source associated with frontal
406 weather systems and gradually depleting effect with increasing rainfall amount
407 (Dunkerley, 2014; Germer et al., 2007). The present study in subtropical forests and



408 previous studies in tropical forests and European temperate forests all exhibited variable
409 rainwater chemistry in throughfall and stemflow, both spatially and temporally
410 (Zimmermann et al., 2007; Staelens et al., 2006; Seiler and Matzner, 1995). In fact, the
411 chemical concentration of rainfall redistribution was also affected profoundly by
412 canopy and stem parameters of tree species (Tonello et al., 2021a; Chen et al., 2019).
413 In our study, some differences of TN, TP and K^+ were also found among SF1~SF8 due
414 to tree-species specific effect (Legout et al., 2016; De Schrijver et al., 2007).

415

416 *4.2. Long-term changes of rainfall in forests*

417 At the long-time scale of 22 years, the complexity of forest structure and rainfall
418 amount and their change exacerbated the spatio-temporal variability of throughfall and
419 stemflow. Firstly, interannual variability of forest structure (e.g., canopy coverage, leaf
420 area index) and tree parameters (e.g., height, DBH and CA) made throughfall and
421 stemflow distribution uncertain (Yue et al., 2021). From 2001 to 2022, changes in forest
422 structure were confirmed in all three forests, such as changes in plant density, canopy
423 coverage and LAI (Fig. 8). Throughfall ratio and stemflow ratio in the succession forest
424 systems all varied over time accordingly. Similarly, driven by forest structure (e.g., tree
425 density, species dominance), a six-year dataset from the Brazilian Atlantic Forest
426 showed that the spatial variability of throughfall over time was less stable (Rodrigues
427 et al., 2022). Besides, the variation of stemflow (CV_{SF}) was obviously larger than that
428 of throughfall (CV_{TF}) (Fig. 4), which probably was attributed to the differences of tree
429 species in stemflow (Fig. 3). For a forest succession, a 17 years' study showed that the
430 shift from monoculture Japanese red pine to mixture of red pine, evergreen oak and
431 theaceous tree made stemflow significantly increasing (Iida et al., 2005). Likewise, for
432 the forest succession in Dinghushan area, stemflow ratio in broadleaf forest and mixed
433 forest were both higher than that in tree-monospecific pine forest. High plant density
434 (tree and shrub) and LAI in broadleaf forest and mixed forest conduce to rainwater
435 interception of multi-canopy trees through more leaves and angled branches, which
436 potentially enhanced stemflow (Fig. 8). Indeed, some differences of rainfall
437 redistribution appeared in multi-layered vegetative structure. An experiment on
438 vegetation communities with a complex multi-layered structure found that interception
439 loss from shrubs was two-times higher than from trees, and smaller trees generated
440 stemflow more efficiently than the higher ones (Exler and Moore, 2022). Based on the
441 22 years' data from forest community survey in our study site, forest canopy parameters



442 (e.g., coverage and LAI) of trees and shrubs showed variation over time from 2001 to
443 2022 (Fig. 8). In the broadleaf forest, plant density of trees and canopy coverage of
444 shrubs showed a slight increment compared to the other two forests, though LAI was
445 decreasing. During this period, interannual throughfall ratio and stemflow ratio showed
446 significantly change over time (Fig. 3), implying the role of interannual variation of
447 forest structure in rainfall redistribution process.

448 Secondly, ongoing rainfall changes with different magnitude favor the different
449 levels of rainfall redistribution over time (Lian et al., 2022). At event scale, throughfall
450 and stemflow proportions of forests were both low with rainfall events <10 mm. The
451 variations of throughfall and stemflow were both larger for gross rainfall <10 mm than
452 events >10 mm. Rainfall threshold associated with the canopy interception capacity had
453 impact on throughfall and stemflow generation (Zabret et al., 2018; André et al., 2008;
454 Durocher, 1990). After the raindrop capacity of the canopy reached its peak, throughfall
455 and stemflow were documented to match the gross rainfall. Therefore, relatively low
456 proportions and high spatial variability appeared before rainfall threshold, and after that,
457 relatively high proportions and low variability until a stable level were observed in the
458 three forests. Moreover, at interannual scale, the raining days in different magnitudes
459 presented obvious fluctuation over 22 years (Fig. 1). This fluctuation of raining days
460 and its magnitude distribution potentially regulated the long-term changes of open
461 rainfall partitioned to interception loss, throughfall and stemflow. Consequently,
462 throughfall and stemflow, influenced by the comprehensive effect of rainfall regimes
463 and forest structures, presented spatiotemporal variability at different level (Fig. 3–6).
464 From a long-term perspective, changing in rainfall redistribution potentially makes
465 forest water and biogeochemistry budget more complex. Further knowledge of the
466 long-term accumulative effect of rainfall redistribution on forest water and chemistry
467 (e.g., soil and plant) is needed in the future.

468

469 **5. Conclusion**

470 The current study investigated long-term changing characteristic of rainfall
471 redistribution along a subtropical forest succession sequence with: pine forest (PF),
472 mixed pine and broadleaf forest (MF) and monsoon evergreen broadleaf forest (BF).
473 Firstly, in the valid 740 rainfall events throughfall ratio showed in order $BF < MF < PF$,
474 and stemflow ratio showed in order $BF > MF > PF$. The variation of stemflow was
475 higher ($CV > 50\%$) than that of throughfall ($CV < 25\%$). Secondly, 22 years' monitored



476 data showed that throughfall ratio widely changed between 30% and 90%, and
477 stemflow ratio changed between 0.1% and 10%. Annual gross rainfall considerably
478 changed over time, which directly induced the variable accumulation of annual
479 throughfall and annual stemflow.

480 For rainwater chemistry, stemflow was characterized with high TN, TP and K^+
481 concentrations compared to throughfall followed by open rainfall. Rainwater chemical
482 concentrations were lower in the rainy season than that in the dry season. However,
483 throughfall, characterized with high fluxes compared to open rainfall followed by
484 stemflow, is the largest contributor to wet deposition. Additionally, differences of the
485 rainwater chemical concentrations among the three forest types were confirmed over
486 time based on data from 2001, 2010 and 2022. On average, TN and TP fluxes of
487 throughfall presented in order $BF < MF < PF$, while K^+ flux of throughfall presented in
488 order $BF > MF > PF$.

489 The above results indicate that the water volume and chemistry in rainfall
490 redistribution process under forest are variable over time, and throughfall and stemflow
491 depend on the effect of rainfall and forest factors. This study thus provided insight into
492 the rainfall redistribution process by linking the long-term change of rainfall pattern
493 with a subtropical forest succession sequence.

494

495

496 *Code and data availability.* The data used to derive to the conclusions of the present
497 study are freely accessible. All the data were obtained from the CNERN dataset
498 (<http://dhf.cern.ac.cn/meta/metaData>).

499

500 *Author contributions.* WJZ: conceptualization, investigation, data analysis, writing,
501 visualization. TS and SS: reviewing, supervision. QMZ and CGW: resources, data
502 curation, WLH: reviewing, JXL: reviewing, funding acquisition, supervision

503

504 *Competing interests.* The authors declare that they have no conflict of interest.

505

506 *Disclaimer.* Publisher's note: Copernicus Publications remains neutral with regard to
507 jurisdictional claims made in the text, published maps, institutional affiliations, or any
508 other geographical representation in this paper. While Copernicus Publications makes
509 every effort to include appropriate place names, the final responsibility lies with the



510 authors.

511

512 *Acknowledgements.* Wanjun Zhang would like to acknowledge the financial support
513 from the CSC Fellowship.

514

515 *Financial support.* This research has been supported by The Key-Area Research and
516 Development Program of Guangdong Province (Grant No. 2022B1111230001), the
517 National Natural Science Foundation of China (Grant Nos. 42207158 and 32101342)
518 and the China Postdoctoral Science Foundation (Grant Nos. 2021M703259, 2021
519 M703260, 2021M693220).

520

521

522 **References**

523 André, F., Jonard, M., Jonard, F., Ponette, Q., 2011. Spatial and temporal patterns of throughfall volume
524 in a deciduous mixed-species stand. *J. Hydrol.* 400(1–2), 244–254.
525 <https://doi.org/10.1016/j.jhydrol.2011.01.037>

526 André, F., Jonard, M., Ponette, Q. (2008). Influence of species and rain event characteristics on stemflow
527 volume in a temperate mixed oak–beech stand. *Hydrol. Process.* 22(22), 4455–4466.
528 <https://doi.org/10.1002/hyp.7048>

529 Blume, T., Schneider, L., Güntner, A., 2022. Comparative analysis of throughfall observations in six
530 different forest stands: Influence of seasons, rainfall-and stand characteristics. *Hydrol. Process.*
531 36(3), e14461. <https://doi.org/10.1002/hyp.14461>

532 Borghetti, M., Gentilesca, T., Leonardi, S., Van Noije, T., Rita, A., 2017. Long-term temporal
533 relationships between environmental conditions and xylem functional traits: a meta-analysis across
534 a range of woody species along climatic and nitrogen deposition gradients. *Tree Physiol.* 37(1), 4–
535 17.

536 Brasil, J.B., Andrade, E.M.d., Palácio, H.A.d.Q., Medeiros, P.H.A., Santos, J.C.N.d., 2018.
537 Characteristics of precipitation and the process of interception in a seasonally dry tropical forest. *J.*
538 *Hydrol-Reg. Stud.* 19, 307–317. <https://doi.org/10.1016/j.ejrh.2018.10.006>

539 Brauman, K.A., Freyberg, D.L., Daily, G.C., 2010. Forest structure influences on rainfall partitioning
540 and cloud interception: A comparison of native forest sites in Kona, Hawai'i. *Agric. For. Meteorol.*
541 150(2), 265–275. <https://doi.org/10.1016/j.agrformet.2009.11.011>

542 Bruijnzeel, L.A., Mulligan, M., Scatena, F.N., 2011. Hydrometeorology of tropical montane cloud forests:
543 emerging patterns. *Hydrol. Process.* 25(3), 465–498. <https://doi.org/10.1002/hyp.7974>

544 Carlyle-Moses, D.E., Laureano, J.F., Price, A.G., 2004. Throughfall and throughfall spatial variability in
545 Madrean oak forest communities of northeastern Mexico. *J. Hydrol.* 297(1–4), 124–135.
546 <https://doi.org/10.1016/j.jhydrol.2004.04.007>

547 Chen, S., Cao, R., Yoshitake, S., Ohtsuka, T., 2019. Stemflow hydrology and DOM flux in relation to



- 548 tree size and rainfall event characteristics. *Agric. For. Meteorol.* 279, 107753.
549 <https://doi.org/10.1016/j.agrformet.2019.107753>
- 550 Crockford, R.H., Richardson, D.P., 1990. Partitioning of rainfall in a eucalypt forest and pine plantation
551 in southeastern Australia: II Stemflow and factors affecting stemflow in a dry sclerophyll eucalypt
552 forest and a *Pinus radiata* plantation. *Hydrol. Process.* 4(2), 145–155.
553 <https://doi.org/10.1002/hyp.3360040205>
- 554 De Schrijver, A., Geudens, G., Augusto, L., Staelens, J., Mertens, J., Wuyts, K., Gielis, L., Verheyen, K.
555 (2007). The effect of forest type on throughfall deposition and seepage flux: a review. *Oecologia*,
556 153, 663–674. <https://doi.org/10.1007/s00442-007-0776-1>
- 557 Dunkerley, D., 2014. Stemflow on the woody parts of plants: dependence on rainfall intensity and event
558 profile from laboratory simulations. *Hydrol. Process.* 28(22), 5469–5482.
559 <https://doi.org/10.1002/hyp.10050>
- 560 Durocher, M.G., 1990. Monitoring spatial variability of forest interception. *Hydrol. Process.* 4(3), 215–
561 229. <https://doi.org/10.1002/hyp.3360040303>
- 562 Exler, J.L., Moore, R.D., 2022. Quantifying throughfall, stemflow and interception loss in five vegetation
563 communities in a maritime raised bog. *Agric. For. Meteorol.* 327, 109202.
564 <https://doi.org/10.1016/j.agrformet.2022.109202>
- 565 Fan, Y.X., Lu, S.X., He, M., Yang, L.M., Hu, W.F., Yang, Z.J., Liu, X.F., Hui, D.F., Guo, J.F., Yang, Y.S.,
566 2021. Long-term throughfall exclusion decreases soil organic phosphorus associated with reduced
567 plant roots and soil microbial biomass in a subtropical forest. *Geoderma*, 404, 115309.
568 <https://doi.org/10.1016/j.geoderma.2021.115309>
- 569 Germer, S., Elsenbeer, H., Moraes, J.M., 2006. Throughfall and temporal trends of rainfall redistribution
570 in an open tropical rainforest, south-western Amazonia (Rondônia, Brazil). *Hydrol. Earth Syst. Sci.*
571 10(3), 383–393. <https://doi.org/10.5194/hess-10-383-2006>
- 572 Germer, S., Neill, C., Krusche, A.V., Neto, S.C.G., Elsenbeer, H., 2007. Seasonal and within-event
573 dynamics of rainfall and throughfall chemistry in an open tropical rainforest in Rondônia, Brazil.
574 *Biogeochemistry*, 86, 155–174. <https://doi.org/10.1007/s10533-007-9152-9>
- 575 Germer, S., Werther, L., Elsenbeer, H., 2010. Have we underestimated stemflow? Lessons from an open
576 tropical rainforest. *J. Hydrol.* 395(3–4), 169–179. <https://doi.org/10.1016/j.jhydrol.2010.10.022>
- 577 Goebes, P., Bruelheide, H., Härdtle, W., Kröber, W., Kühn, P., Li, Y., Seitz, S., von Oheimb, G., Scholten,
578 T., 2015. Species-specific effects on throughfall kinetic energy in subtropical forest plantations are
579 related to leaf traits and tree architecture. *PLoS one*, 10(6), e0128084.
580 <https://doi.org/10.1371/journal.pone.0128084>
- 581 Grunicke, S., Queck, R., Bernhofer, C., 2020. Long-term investigation of forest canopy rainfall
582 interception for a spruce stand. *Agric. For. Meteorol.* 292, 108125.
583 <https://doi.org/10.1016/j.agrformet.2020.108125>
- 584 Grossiord, C., Sevanto, S., Dawson, T. E., Adams, H.D., Collins, A.D., Dickman, L.T., Newman B.D.,
585 Stockton, E.A., McDowell, N.G. (2017). Warming combined with more extreme precipitation
586 regimes modifies the water sources used by trees. *New Phytol.* 213(2), 584–596.
587 <https://doi.org/10.1111/nph.14192>



- 588 Huang, W.J., Zhou, G.Y., Liu, J.X., 2012. Nitrogen and phosphorus status and their influence on
589 aboveground production under increasing nitrogen deposition in three successional forests. *Acta*
590 *Oecologica*, 44, 20–27. <https://doi.org/10.1016/j.actao.2011.06.005>
- 591 Iida, S.I., Tanaka, T., Sugita, M., 2005. Change of interception process due to the succession from
592 Japanese red pine to evergreen oak. *J. Hydrol.* 315(1–4), 154–166.
593 <https://doi.org/10.1016/j.jhydrol.2005.03.024>
- 594 Jackson, N.A., 2000. Measured and modelled rainfall interception loss from an agroforestry system in
595 Kenya. *Agric. For. Meteorol.* 100, 323–336. [https://doi.org/10.1016/S0168-1923\(99\)00145-8](https://doi.org/10.1016/S0168-1923(99)00145-8)
- 596 Ji, S.Y., Omar, S.I., Zhang, S.B., Wang, T.F., Chen, C.F., Zhang, W.J., 2022. Comprehensive evaluation of
597 throughfall erosion in the banana plantation. *Earth Surf. Proc. Land.*, 47(12), 2941–2949.
598 <https://doi.org/10.1002/esp.5435>
- 599 Jiang, Z.Y., Zhi, Q.Y., Van Stan, J.T., Zhang, S.Y., Xiao, Y.H., Chen, X.Y., Wu, H.W., 2021. Rainfall
600 partitioning and associated chemical alteration in three subtropical urban tree species. *J. Hydrol.*
601 603, 127109. <https://doi.org/10.1016/j.jhydrol.2021.127109>
- 602 Junior, J.J., Mello, C.R., Owens, P.R., Mello, J.M., Curi, N., Alves, G.J., 2017. Time-stability of soil
603 water content (SWC) in an Atlantic Forest-Latosol site. *Geoderma*, 288, 64–78.
604 <https://doi.org/10.1016/j.geoderma.2016.10.034>
- 605 Keim, R.F., Tromp-van Meerveld, H.J., McDonnell, J.J., 2006. A virtual experiment on the effects of
606 evaporation and intensity smoothing by canopy interception on subsurface stormflow generation. *J.*
607 *Hydrol.* 327(3–4), 352–364. <https://doi.org/10.1016/j.jhydrol.2005.11.024>
- 608 Klos, P.Z., Chain-Guadarrama, A., Link, T.E., Finegan, B., Vierling, L.A., Chazdon, R., 2014.
609 Throughfall heterogeneity in tropical forested landscapes as a focal mechanism for deep percolation.
610 *J. Hydrol.* 519, 2180–2188. <https://doi.org/10.1016/j.jhydrol.2014.10.004>
- 611 Kottek, M., Grieser, J., Beck, C., Rudolf, B., Rubel, F., 2006. World map of the Köppen-Geiger climate
612 classification updated. *Meteorologische Zeitschrift*, 15(3), 259–263. [https://doi.org/10.1127/0941-](https://doi.org/10.1127/0941-2948/2006/0130)
613 [2948/2006/0130](https://doi.org/10.1127/0941-2948/2006/0130)
- 614 Lacombe, G., Valentin, C., Sounyafong, P., De Rouw, A., Souleuth, B., Silvera, N., Pierret, A.,
615 Sengtaheuanghong, O., Ribolzi, O., 2018. Linking crop structure, throughfall, soil surface
616 conditions, runoff and soil detachment: 10 land uses analyzed in Northern Laos. *Sci. Total Environ.*
617 616, 1330–1338. <https://doi.org/10.1016/j.scitotenv.2017.10.185>
- 618 Legout, A., van Der Heijden, G., Jaffrain, J., Boudot, J. P., Ranger, J., 2016. Tree species effects on
619 solution chemistry and major element fluxes: A case study in the Morvan (Breuil, France). *Forest*
620 *Ecol Manag.* 378, 244–258. <https://doi.org/10.1016/j.foreco.2016.07.003>
- 621 Leuzinger, S., Körner, C., 2010. Rainfall distribution is the main driver of runoff under future CO₂-
622 concentration in a temperate deciduous forest. *Global Change Biol.* 16(1), 246–254.
623 <https://doi.org/10.1111/j.1365-2486.2009.01937.x>
- 624 Levia, D.F., Nanko, K., Amasaki, H., Giambelluca, T. W., Hotta, N., Iida, S. I., Mudd, R.G., Nullet, M.A.,
625 Sakai, N., Shinori, Y., Sun X.C., Suzuki, M., Tanaka, N., Tantasirin, C., Yamada, K., 2019.
626 Throughfall partitioning by trees. *Hydrol. Process.* 33(12), 1698–1708.
627 <https://doi.org/10.1002/hyp.13432>



- 628 Levia, D.F., Germer, S., 2015. A review of stemflow generation dynamics and stemflow-environment
629 interactions in forests and shrublands. *Rev. Geophys.* 53(3), 673–714.
630 <https://doi.org/10.1002/2015RG000479>
- 631 Levia Jr, D.F., Frost, E.E., 2006. Variability of throughfall volume and solute inputs in wooded
632 ecosystems. *Prog. Phys. Geog.* 30(5), 605–632. <https://doi.org/10.1177/0309133306071145>
- 633 Li, Y., Niu, S.L., Yu, G.R., 2016. Aggravated phosphorus limitation on biomass production under
634 increasing nitrogen loading: a meta-analysis. *Global Change Biol.* 22(2), 934–943.
635 <https://doi.org/10.1111/gcb.13125>
- 636 Lian, X., Zhao, W.L., Gentine, P., 2022. Recent global decline in rainfall interception loss due to altered
637 rainfall regimes. *Nat. Commun.* 13(1), 7642. <https://doi.org/10.1038/s41467-022-35414-y>
- 638 Liu, J.Q., Liu, W.J., Li, W.X., Zeng, H.H., 2019. How does a rubber plantation affect the spatial variability
639 and temporal stability of throughfall? *Hydrol. Res.* 50(1), 60–74.
640 <https://doi.org/10.2166/nh.2018.028>
- 641 Livesley, S.J., Baudinette, B., Glover, D., 2014. Rainfall interception and stem flow by eucalypt street
642 trees – The impacts of canopy density and bark type. *Urban For. Urban Gree.* 13(1), 192–197.
643 <https://doi.org/10.1016/j.ufug.2013.09.001>
- 644 Llorens, P., Domingo, F., 2007. Rainfall partitioning by vegetation under Mediterranean conditions. A
645 review of studies in Europe. *J. Hydrol.* 335(1–2), 37–54.
646 <https://doi.org/10.1016/j.jhydrol.2006.10.032>
- 647 Llorens, P., Latron, J., Carlyle-Moses, D.E., Nätthe, K., Chang, J.L., Nanko, K., Lida, S., Levia, D.F.,
648 2022. Stemflow infiltration areas into forest soils around American beech (*Fagus grandifolia* Ehrh.)
649 trees. *Ecohydrology* 15(2), e2369. <https://doi.org/10.1002/eco.2369>
- 650 Loustau, D., Berbigier, P., Granier, A., 1992. Interception loss, throughfall and stemflow in a maritime
651 pine stand. II. An application of Gash's analytical model of interception. *J. Hydrol.* 138(3–4), 469–
652 485. [https://doi.org/10.1016/0022-1694\(92\)90131-E](https://doi.org/10.1016/0022-1694(92)90131-E)
- 653 Marin, C.T., Bouten, W., Sevink, J., 2000. Gross rainfall and its partitioning into throughfall, stemflow
654 and evaporation of intercepted water in four forest ecosystems in western Amazonia. *J. Hydrol.*
655 237(1–2), 40–57. [https://doi.org/10.1016/S0022-1694\(00\)00301-2](https://doi.org/10.1016/S0022-1694(00)00301-2)
- 656 Moslehi, M., Habashi, H., Khormali, F., Ahmadi, A., Brunner, I., Zimmermann, S., 2019. Base cation
657 dynamics in rainfall, throughfall, litterflow and soil solution under Oriental beech (*Fagus orientalis*
658 Lipsky) trees in northern Iran. *Ann. Forest Sci.* 76(2), 1–12. <https://doi.org/10.1007/s13595-019-0837-8>
- 659 0837-8
- 660 Muzyło, A., Llorens, P., Domingo, F., 2012. Rainfall partitioning in a deciduous forest plot in leafed and
661 leafless periods. *Ecohydrology*, 5(6), 759–767. <https://doi.org/10.1002/eco.266>
- 662 Nanko, K., Hotta, N., Suzuki, M., 2006. Evaluating the influence of canopy species and meteorological
663 factors on throughfall drop size distribution. *J. Hydrol.* 329(3–4), 422–431.
664 <https://doi.org/10.1016/j.jhydrol.2006.02.036>
- 665 Niu, X.T., Fan, J., Du, M.G., Dai, Z.J., Luo, R.H., Yuan, H.Y., Zhang, S.G., 2023. Changes of Rainfall
666 Partitioning and canopy interception modeling after progressive thinning in two shrub plantations
667 on the Chinese Loess Plateau. *J. Hydrol.* 619, 129299.



- 668 <https://doi.org/10.1016/j.jhydrol.2023.129299>
- 669 Ponette-González, A.G., Weathers, K.C., Curran, L.M., 2010. Water inputs across a tropical montane
670 landscape in Veracruz, Mexico: synergistic effects of land cover, rain and fog seasonality, and
671 interannual precipitation variability. *Global Change Biol.* 16(3), 946–963.
672 <https://doi.org/10.1111/j.1365-2486.2009.01985.x>
- 673 Price, A.G., Dunham, K., Carleton, T., Band, L., 1997. Variability of water fluxes through the black
674 spruce (*Picea mariana*) canopy and feather moss (*Pleurozium schreberi*) carpet in the boreal forest
675 of Northern Manitoba. *J. Hydrol.* 196(1–4), 310–323. [https://doi.org/10.1016/S0022-1694\(96\)03233-7](https://doi.org/10.1016/S0022-1694(96)03233-7)
- 676
- 677 Reynaert, S., De Boeck, H.J., Verbruggen, E., Verlinden, M., Flowers, N., Nijs, I., 2021. Risk of short-
678 term biodiversity loss under more persistent precipitation regimes. *Global Change Biol.* 27(8),
679 1614–1626. <https://doi.org/10.1111/gcb.15501>
- 680 Rodrigues, A.F., Terra, M.C., Mantovani, V.A., Cordeiro, N.G., Ribeiro, J.P., Guo, L., Nehren, U., Mello,
681 M.J., Mello, C.R., 2022. Throughfall spatial variability in a neotropical forest: Have we correctly
682 accounted for time stability? *J. Hydrol.* 608, 127632. <https://doi.org/10.1016/j.jhydrol.2022.127632>
- 683 Seiler, J., Matzner, E., 1995. Spatial variability of throughfall chemistry and selected soil properties as
684 influenced by stem distance in a mature Norway spruce (*Picea abies*, Karst.) stand. *Plant Soil* 176,
685 139–147. <https://doi.org/10.1007/BF00017684>
- 686 Shen, W.J., Ren, H.L., Jenerette, G.D., Hui, D.F., Ren, H., 2013. Atmospheric deposition and canopy
687 exchange of anions and cations in two plantation forests under acid rain influence. *Atmos Environ.*
688 64, 242–250. <https://doi.org/10.1016/j.atmosenv.2012.10.015>
- 689 Shinohara, Y., Levia, D.F., Komatsu, H., Nogata, M., Otsuki, K., 2015. Comparative modeling of the
690 effects of intensive thinning on canopy interception loss in a Japanese cedar (*Cryptomeria japonica*
691 D. Don) forest of western Japan. *Agric. For. Meteorol.* 214–215, 148–156.
692 <https://doi.org/10.1016/j.agrformet.2015.08.257>.
- 693 Siegert, C.M., Levia, D.F., 2014. Seasonal and meteorological effects on differential stemflow funneling
694 ratios for two deciduous tree species. *J. Hydrol.* 519, 446–454.
695 <https://doi.org/10.1016/j.jhydrol.2014.07.038>
- 696 Staelens, J., De Schrijver, A., Verheyen, K., 2007. Seasonal variation in throughfall and stemflow
697 chemistry beneath a European beech (*Fagus sylvatica*) tree in relation to canopy phenology. *Can. J.*
698 *Forest Res.* 37(8), 1359–1372. <https://doi.org/10.1139/X07-003>
- 699 Staelens, J., De Schrijver, A., Verheyen, K., Verhoest, N.E., 2006. Spatial variability and temporal
700 stability of throughfall deposition under beech (*Fagus sylvatica* L.) in relationship to canopy
701 structure. *Environ. Pollut.* 142(2), 254–263. <https://doi.org/10.1016/j.envpol.2005.10.002>
- 702 Su, L., Zhao, C.M., Xu, W.T., Xie, Z.Q., 2019. Hydrochemical fluxes in bulk precipitation, throughfall,
703 and stemflow in a mixed evergreen and deciduous broadleaved forest. *Forests* 10(6), 507.
704 <https://doi.org/10.3390/f10060507>
- 705 Sun, J.M., Yu, X.X., Wang, H.N., Jia, G.D., Zhao, Y., Tu, Z.H., Deng, W.P., Jia, J.B., Chen, J.G., 2018.
706 Effects of forest structure on hydrological processes in China. *J. Hydrol.* 561, 187–199.
707 <https://doi.org/10.1016/j.jhydrol.2018.04.003>



- 708 Sun, S.Y., Liu, X.F., Lu, S.X., Cao, P.L., Hui, D.F., Chen, J., Guo, J.F., Yang, Y.S., 2023. Depth-dependent
709 response of particulate and mineral-associated organic carbon to long-term throughfall reduction in
710 a subtropical natural forest. *Catena*, 223, 106904. <https://doi.org/10.1016/j.catena.2022.106904>
- 711 Tonello, K.C., Rosa, A.G., Pereira, L.C., Matus, G.N., Guandique, M.E.G., Navarrete, A.A., 2021a.
712 Rainfall partitioning in the Cerrado and its influence on net rainfall nutrient fluxes. *Agric. For.
713 Meteorol.* 303, 108372. <https://doi.org/10.1016/j.agrformet.2021.108372>
- 714 Tonello, K.C., Van Stan II, J.T., Rosa, A.G., Balbinot, L., Pereira, L.C., Bramorski, J., 2021b. Stemflow
715 variability across tree stem and canopy traits in the Brazilian Cerrado. *Agric. For. Meteorol.* 308,
716 108551. <https://doi.org/10.1016/j.agrformet.2021.108551>
- 717 Turpault, M.P., Kirchen, G., Calvaruso, C., Redon, P.O., Dincher, M., 2021. Exchanges of major elements
718 in a deciduous forest canopy. *Biogeochemistry*, 152, 51–71. [https://doi.org/10.1007/s10533-020-
00732-0](https://doi.org/10.1007/s10533-020-
719 00732-0)
- 720 Wu, T., Song, Y.T., Tissue, D., Su, W., Luo, H.Y., Li, X., Yang, S.M., Liu, X.J., Yan J.H., Huang, J., Liu,
721 J.X., 2023. Photosynthetic and biochemical responses of four subtropical tree seedlings to reduced
722 dry season and increased wet season precipitation and variable N deposition. *Tree Physiol.* tpad114.
- 723 Van Stan II, J.T., Pypker, T.G., 2015. A review and evaluation of forest canopy epiphyte roles in the
724 partitioning and chemical alteration of precipitation. *Sci. Total Environ.* 536, 813–824.
725 <https://doi.org/10.1016/j.scitotenv.2015.07.134>
- 726 Van Stan, J.T., Wagner, S., Guillemette, F., Whitetree, A., Lewis, J., Silva, L., Stubbins, A., 2017.
727 Temporal dynamics in the concentration, flux, and optical properties of tree-derived dissolved
728 organic matter in an epiphyte-laden oak-cedar forest. *J. Geophys. Res-Biogeophys.* 122(11), 2982–2997.
729 <https://doi.org/10.1002/2017JG004111>
- 730 Wang, C.Y., Sun, X.C., Fan, C.B., Wei, Y.X., Jia, G.K., Cao, Y.H., 2023. Spatio-temporal variability and
731 intra-event variation of throughfall ammonium and nitrate in a pine plantation. *Hydrol. Process.*
732 e14872. <https://doi.org/10.1002/hyp.14872>
- 733 Yan, J.H., Zhou, G.Y., Zhang, D.Q., Wang, X., 2003. Spatial and temporal variations of some
734 hydrological factors in a climax forest ecosystem in the Dinghushan region. *Acta Ecologica Sinica*
735 23(11), 2359–2366. <https://europaemc.org/article/cba/534217>
- 736 Yue, K., De Frenne, P., Fornara, D.A., Van Meerbeek, K., Li, W., Peng, X., Ni, X.Y., Peng, Y., Wu, F.Z.,
737 Yang Y.S., Peñuelas, J., 2021. Global patterns and drivers of rainfall partitioning by trees and
738 shrubs. *Global Change Biol.* 27(14), 3350–3357. <https://doi.org/10.1111/gcb.15644>
- 739 Zabret, K., Rakovec, J., Šraj, M., 2018. Influence of meteorological variables on rainfall partitioning for
740 deciduous and coniferous tree species in urban area. *J. Hydrol.* 558, 29–41.
741 <https://doi.org/10.1016/j.jhydrol.2018.01.025>
- 742 Zhang, W.J., Zhu, X.A., Chen, C.F., Zeng, H.H., Jiang, X.J., Wu, J.E., Zou, X., Yang, B., Liu, W.J., 2021.
743 Large broad-leaved canopy of banana (*Musa nana* Lour.) induces dramatically high spatial–
744 temporal variability of throughfall. *Hydrol. Res.* 52(6), 1223–1238.
745 <https://doi.org/10.2166/nh.2021.023>
- 746 Zhang, Y.F., Wang, X.P., Hu, R., Pan, Y.X., Paradeloc, M., 2015. Rainfall partitioning into throughfall,
747 stemflow and interception loss by two xerophytic shrubs within a rain-fed re-vegetated desert



- 748 ecosystem, northwestern China. J. Hydrol. 527, 1084–1095.
749 <https://doi.org/10.1016/j.jhydrol.2015.05.060>
- 750 Zhang, Y.F., Yuan, C., Chen, N., Levia, D.F., 2023. Rainfall partitioning by vegetation in China: A
751 quantitative synthesis. J. Hydrol. 617, 128946. <https://doi.org/10.1016/j.jhydrol.2022.128946>
- 752 Zhao, W.Y., Ji, X.B., Jin, B.W., Du, Z.Y., Zhang, J.L., Jiao, D.D., Zhao, L.W., 2023. Experimental
753 partitioning of rainfall into throughfall, stemflow and interception loss by *Haloxylon ammodendron*,
754 a dominant sand-stabilizing shrub in northwestern China. Sci. Total Environ. 858, 159928.
755 <https://doi.org/10.1016/j.scitotenv.2022.159928>
- 756 Zheng, M.H., Zhang, T., Luo, Y.Q., Liu, J.X., Lu, X.K., Ye, Q., Wang, S.H., Huang, J., Mao, Q.G., Mo,
757 J.M., Zhang, W., 2022. Temporal patterns of soil carbon emission in tropical forests under long-term
758 nitrogen deposition. Nat. Geosci. 15, 1002–1010. <https://doi.org/10.1038/s41561-022-01080-4>
- 759 Zhou, G.Y., Wei, X.H., Wu, Y.P., Liu, S.G., Huang, Y.H., Yan, J.H., Zhang, D.Q., Zhang, Q.M., Liu, J.X.,
760 Meng, Z., Wang, C.L., Chu, G.W., Liu, S.Z., Tang, X.L., Liu, X.D., 2011. Quantifying the
761 hydrological responses to climate change in an intact forested small watershed in Southern China.
762 Global Change Biol. 17(12), 3736–3746. <https://doi.org/10.1111/j.1365-2486.2011.02499.x>
- 763 Ziegler, A.D., Giambelluca, T.W., Nullet, M.A., Sutherland, R.A., Tantasarin, C., Vogler, J.B., Negishi,
764 J.N., 2009. Throughfall in an evergreen-dominated forest stand in Northern Thailand: comparison
765 of mobile and stationary methods. Agric. For. Meteorol. 149, 373–384.
766 <https://doi.org/10.1016/j.agrformet.2008.09.002>.
- 767 Zimmermann, A., Wilcke, W., Elsenbeer, H., 2007. Spatial and temporal patterns of throughfall quantity
768 and quality in a tropical montane forest in Ecuador. J. hydrol. 343(1–2), 80–96.
769 <https://doi.org/10.1016/j.jhydrol.2007.06.012>



770 **Tables**

771

772 **Table 1** Correlations between throughfall and stemflow and rainfall and forest factors

	Gross rainfall	DBH	CA	Height	LAI
Throughfall	0.72***	—	—	—	-0.58**
stemflow	0.77***	0.65*	-0.75**	0.54**	-0.55**

773 DBH: diameter at breast height; CA: crown area; LAI: leaf area index. * $P < 0.05$, ** $P < 0.01$, *** $P <$

774 0.001

775

776

777

778

779

780

781 **Table 2** Analysis of variance (ANOVA) for throughfall and stemflow affected by rainfall
 782 classifications and tree species

Summary of ANOVA	Throughfall		Stemflow
Rainfall classification (R)	< 0.05	Rainfall classification (R)	< 0.001
Forest type (F)	< 0.001	Tree species (T)	< 0.001
R × F	0.861	R × T	< 0.001

783 $\alpha = 0.05$

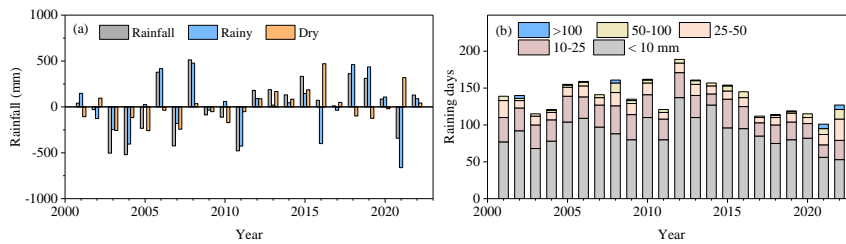
784



785 **Figures**

786

787

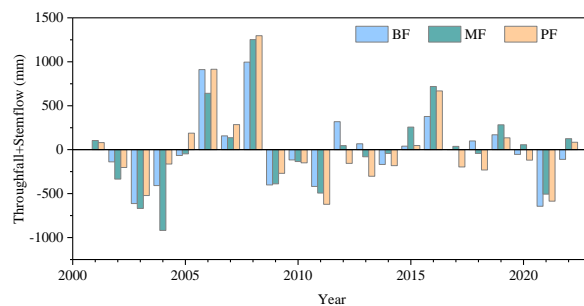


788

789 **Fig. 1** (a) Anomaly of annual rainfall from 2001–2022 at the Dinghushan Biosphere Reserve in
790 southern China, (b) annual raining days in five classifications



791



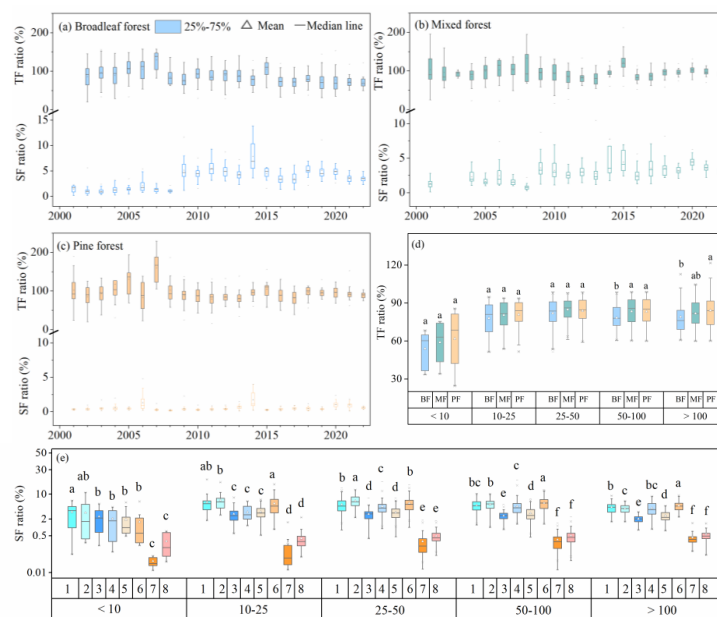
792

793

Fig. 2 Anomaly of annual rainfall redistribution (throughfall + stemflow) in the broadleaf forest

794

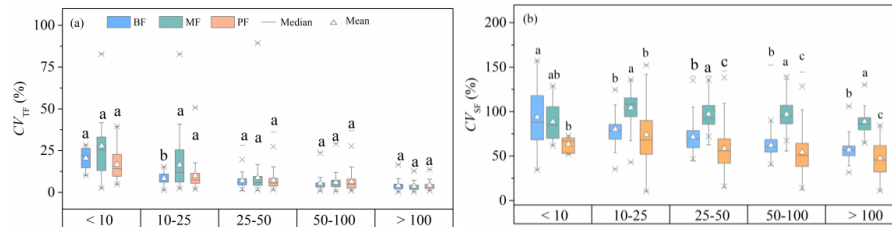
(BF), mixed pine and broadleaf forest (MF) and pine forest (PF) from 2001–2022



795
 796 **Fig. 3** Box plots of throughfall ratio and stemflow ratio in (a) broadleaf forest, (b) mixed pine and
 797 broadleaf forest and (c) pine forest from 2001–2022. Boxed plots of (d) TF ratio in the three
 798 forests and (e) SF ratio for eight plant species based on the rainfall classifications (broadleaf
 799 forest: *Acmena acuminatissima* (Blume) Merr. et Perry (SF1), *Cryptocarya chinensis* (Hance)
 800 Hemsl. (SF2), *Gironniera subaequalis* Planch. (SF3), *Schima superba* Gardn. et Champ. (SF4);
 801 mixed forest: *Castanea henryi* (Skam) Rehd. et Wils. (SF5), *Schima superba* Gardn. et Champ.
 802 (SF6), *Pinus massoniana* Lamb. (SF7); pine forest: *Pinus massoniana* Lamb. (SF8). Different
 803 letters indicate a significant difference at $P < 0.05$



804



805

806

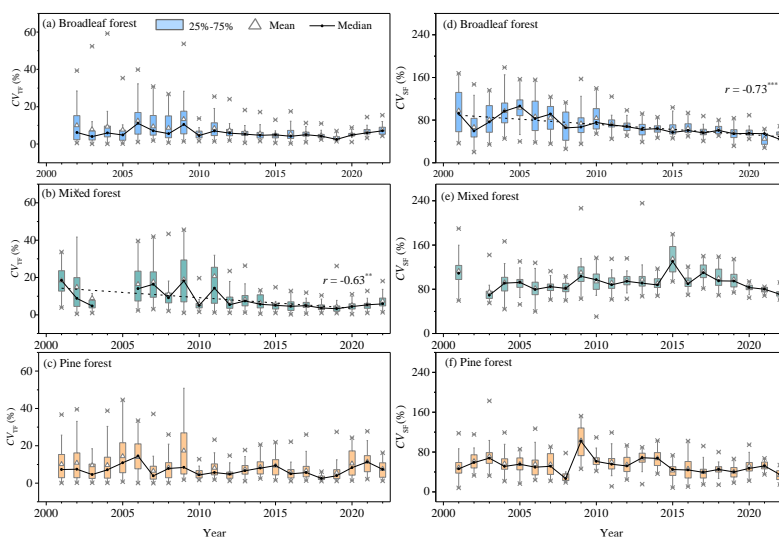
807

808

Fig. 4 Box plots of coefficient of variation (CV , %) in (a) throughfall (TF) and (b) stemflow (SF) in broadleaf forest (BF), mixed pine and broadleaf forest (MF) and pine forest (PF) based on the rainfall classifications. Different letters indicate a significant difference at $P < 0.05$



809

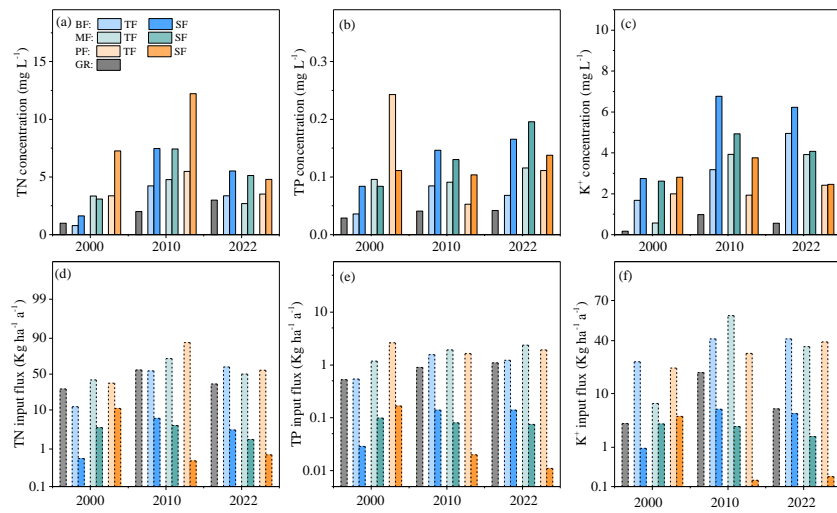


810

811 **Fig. 5** Box plots of coefficient of variation (CV , %) in (a, b, and c) throughfall (TF) and (d, e, and f)

812 stemflow (SF) in the three forests from 2001 to 2022. Medians of annual CV were fitted. r :

813 Pearson coefficient of correlation; *: $P < 0.05$, **: $P < 0.01$, ***: $P < 0.001$



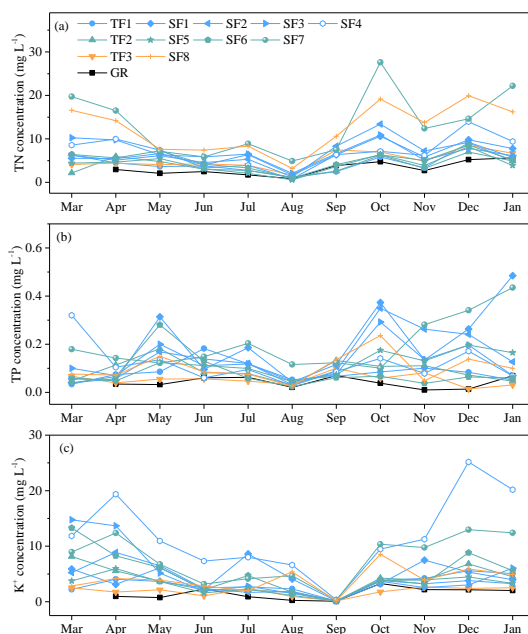
814

815

816

817

Fig. 6 Concentrations and fluxes of TN, TP and K⁺ of gross rainfall (GR), throughfall (TF) and stemflow (SF) in the broadleaf forest (BF), mixed forest (MF) and pine forest (PF) in 2000, 2010 and 2022, respectively.



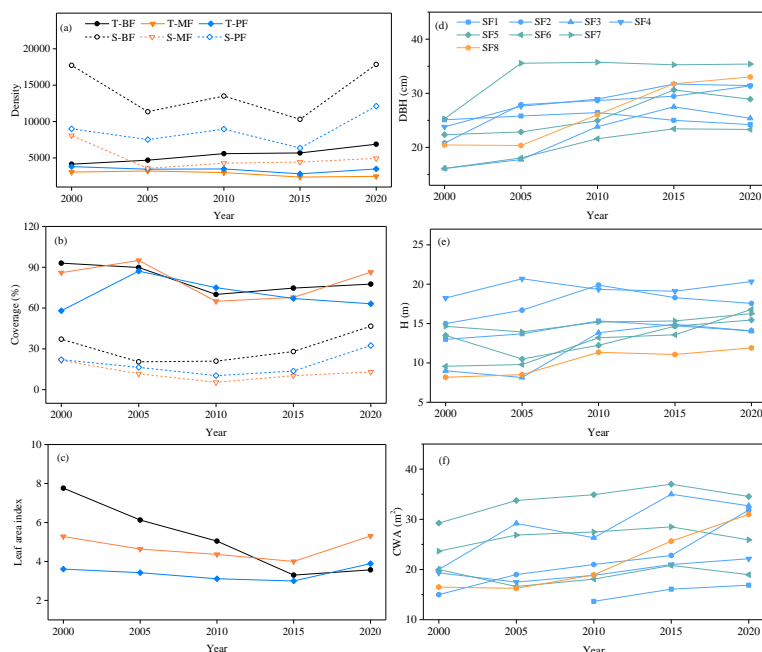
818

819

820

821

Fig. 7 Monthly concentrations of (a) TN, (b) TP and (c) K⁺ of throughfall (TF1, SF2, SF3 and SF4) in the broadleaf forest, throughfall (TF2) and stemflow (SF5, SF6 and SF7) in the mixed forest, throughfall (TF3) and stemflow (SF8) in the pine forest.



822
823 **Fig. 8** Plant density, canopy coverage and leaf area index of tree (T) and shrub (S) in the broadleaf
824 forest (BF), mixed forest (MF) and pine forest (PF), respectively. Diameter at breast height
825 (DBH), height (H) and crown area (CA) is given for eight stemflow-sampled trees, respectively.